

1 **Influences of Solution Plasma Conditions on Degradation Rate and**  
2 **Properties of Chitosan**

3 Tantiplapol T.<sup>1</sup>, Singsawat Y.<sup>1</sup>, Narongsil N.<sup>1</sup>, Damrongsakkul S.<sup>2,3</sup>, Saito N.<sup>4</sup>, and  
4 Prasertsung I.<sup>1,3\*</sup>

5 <sup>1</sup>Chemical Engineering Program, Department of Industrial Engineering, Faculty of  
6 Engineering, Naresuan University, Phitsanulok 65000, Thailand

7 <sup>2</sup>Department of Chemical Engineering, Faculty of Engineering, Chulalongkorn  
8 University, Bangkok 10330, Thailand

9 <sup>3</sup>Plasma Technology and Nuclear Fusion Research Unit, Chulalongkorn University,  
10 Bangkok 10330, Thailand

11 <sup>3</sup>Reaction Kinetics and Dynamics Research Group, Department of Materials, Physics  
12 and Energy Engineering, Graduate School of Engineering, Nagoya University, Furo-  
13 cho, Chikusa-ku, Nagoya 464-8603, Japan

14 \*Corresponding author. Tel.: +66-5-5964245; Fax: +66-5-5964256. E-mail address:

15 [isarawutp@nu.ac.th](mailto:isarawutp@nu.ac.th)

16

17

18

19

20

21

22

23

24

25

สำเนาถูกต้อง  


**26 Abstract**

27 In this work, the effects of solution plasma conditions on the degradation rate  
28 and properties of chitosan are investigated. Various types of electrodes including  
29 tungsten (W), copper (Cu), and iron (Fe) were used. The treatment time and the  
30 applied pulse frequency of the bipolar supply varied from 0 to 210 minutes and 15 to  
31 30 kHz, respectively. The plasma-treated chitosan was characterized by GPC, XRD,  
32 FT-IR, and fractionation analysis. The results showed that after plasma treatment for  
33 210 minutes, the molecular weight of chitosan decreased remarkably, when compared  
34 to those of untreated samples. The plasma treatment of chitosan using Fe electrode  
35 and high pulse frequency strongly promoted the degradation rate of chitosan. The  
36 XRD analysis showed that the crystallinity of plasma-treated chitosan was destroyed.  
37 FT-IR analysis revealed that the chemical structure of chitosan was not changed by  
38 solution plasma treatment. Solution plasma treatment of chitosan using an Fe  
39 electrode provided the highest %yield of water-soluble chitosan.

40

**41 Keywords**

42 Solution Plasma Process; Chitosan; Degradation rate

43

44

45

46

47

48

49

50

สำเนาถูกต้อง



## 51 1. Introduction

52 Chitosan, the deacetylated derivative of chitin, is one of the abundant,  
53 nontoxic, renewable, biodegradable polymers. It is composed of  $\beta$ -1,4-linked 2-  
54 amino-2-deoxy-D-glucopyranose (GlcN) and 2-acet-amido-2-deoxy-D-glucopyranose  
55 (GlcNAc) units and widely presented in exoskelatons of shellfish and insect (Shahidi  
56 et al., 1999; Jayakumar et al., 2010; Jayakumar et al., 2011). Therefore, chitosan has  
57 received much attention for various applications such as food, pharmaceutics,  
58 biomaterials, drug delivery, medicine and cosmetics. However, the high molecular  
59 weight, high viscosity, and low solubility in water of chitosan derived from chitin are  
60 the main problems and restrict its application. Several techniques including chemical,  
61 physical and enzymatic treatment have already been performed to degrade the high  
62 molecular weight chitosan into low molecular weight chitosan (LMWC) which  
63 exhibits water solubility, bioactivities including antitumor, antimicrobial as well as  
64 anti-inflammatory properties (Yue et al., 2008; Xie et al., 2009; Choi et al., 2002;  
65 Chang et al., 2001). Among these techniques, enzymatic treatment is an effective  
66 process to achieve LMWC. However, the main drawbacks of this process are low  
67 production yield and slowly enzymatic reaction. In addition, since it is operated  
68 under mild conditions and requires multiple steps, especially enzyme preparation and  
69 product purification, therefore, this process is considered as the complicated and high  
70 cost process.

71 Electrical discharge in the liquid phase is known as "Solution plasma process  
72 (SPP)", and has recently been proposed to be an effective process. Currently, SPP has  
73 received much attention for various applications such as carbon material synthesis,  
74 surface modification of polymers, wastewater treatment, and degradation of organic  
75 compounds (Takai, 2008). An important advantages of SPP is the production of

A handwritten signature in black ink is located at the bottom right of the page. Above the signature is a blue circular stamp containing Thai text, which is partially obscured by the signature.

76 highly active species especially hydroxyl radicals ( $\text{OH}^\bullet$ ) is obtained (Potocký et al.,  
77 2009; Prasertsung et al., 2011; Prasertsung et al., 2013). Moreover, since the solution  
78 plasma is generated under mild conditions and not involved any strong chemical  
79 reagents, therefore the removal of chemical residue is not required. The present study  
80 was aimed to study the effects of SPP conditions on the degradation rate and  
81 properties of the degraded chitosan product. For this purpose, the degradation of  $\beta$ -  
82 chitosan was carried out by SPP with different types of electrodes and the applied  
83 pulse frequency. The degradation rate of chitosan was calculated by kinetic study. The  
84 properties of chitosan including the molecular weight, chemical structure, crystal  
85 structure and solubility were investigated. The properties of degraded products were  
86 characterized by GPC, FT-IR, and XRD. Moreover, the water solubility of degraded  
87 product was then determined by fractional analysis.

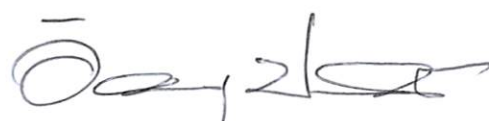
88

## 89 2. Materials and Methods

### 90 2.1 Materials

91  $\beta$ -Chitosan was prepared according to a procedure similar to that described by  
92 Sashiwa *et al.* (Sashiwa et al., 2003). In short, the ground squid pen was soaked in 2 N  
93 NaOH solution overnight to deproteinize. The deproteinized product were then treated  
94 with a similar solution at 100°C for 4 h followed by excessive washing with distilled  
95 water to remove more residual protein. The  $\beta$ -chitin samples were deacetylated with  
96 25% NaOH (112.5°C) to achieve  $\beta$ -Chitosan with the degree of deacetylation and  
97 average molecular weight of 90% and  $1.3 \times 10^5$  Da, respectively. Acetic acid, acetone,  
98 hydrochloric acid, and sodium hydroxide were used as received. All of the chemicals,  
99 reagents, and solvents used were of analytical grades. The water used was distilled  
100 and deionized.

สำเนาถูกต้อง





## 101 2.2 Solution plasma experiment

102  $\beta$ -Chitosan was dissolved in 1 M acetic acid to obtain 0.5% w/v chitosan  
103 solution and placed in the glass reactor. The setup of solution plasma system,  
104 modified from our previous study (Prasertsung et al., 2013), is shown in Figure 1. The  
105 solution plasma was operated at atmospheric pressure. The solution plasma was  
106 produced at the fixed voltage and pulse width of 1.6 kV and 2  $\mu$ s, respectively.  
107 Various types of electrodes including tungsten (W), copper (Cu) and iron (Fe) were  
108 used. The applied pulse frequency of bipolar power supply and treatment time of the  
109 solution plasma were within the ranges of 15-30 kHz and 0-210 minutes, respectively.  
110 The uniformity of chitosan solution to contact with the plasma was controlled using  
111 magnetic stirrer. After the plasma treatment of chitosan was completed, the plasma-  
112 treated and untreated chitosan were characterized.

113

## 114 2.3 Characterization of plasma-treated chitosan

115 Optical emission spectroscopy (OES) was used to monitor the light emitted  
116 from the plasma in the wavelength range of 200–1000 nm. To characterize the species  
117 in plasma-treated chitosan solutions, the emission was detected through the quartz  
118 glass window with an optical fiber placed 1 mm in front of the glass chamber. Data  
119 was acquired with Avantes software (Baroch et al., 2008).

120 Gel Permeation Chromatography (GPC, Water 600E, Waters, USA) was used  
121 to characterize the apparent molecular weights of plasma-treated and untreated  
122 chitosan solutions. The ultrahydrogel linear 1 column was used. The concentration of  
123 chitosan solutions was 0.4 mg/ml. Eluent and chitosan sample solutions were filtered  
124 through 0.45  $\mu$ m Millipore filters. The flow rate was maintained at 0.6 ml/min at 30°C.  
125 The pullulans ( $M_w$  5900-708000 Da) were used as standard samples.

สำเนาถูกต้อง  


126 The crystal structure of both before and after degradation was characterized by  
127 X-ray diffractometer (Shimadzu Lab XRD-6000, Japan). The plasma-treated and  
128 untreated chitosan solutions were cast into mold to form thin films. X-ray diffraction  
129 patterns of the plasma-treated and untreated chitosan films were measured with a  
130 CuK $\alpha$  target at 40 kV and 50 mA. The relative intensity was recorded in the scattering  
131 range ( $2\theta$ ) of 5-40 $^\circ$ .

132 FT-IR spectroscopy (Digilab, FTS 7000 Series, USA) was used to characterize  
133 the chemical composition of plasma-treated and untreated chitosan samples. All of the  
134 ATR-FTIR spectra were collected using 64 scans in the range of 4000–400  $\text{cm}^{-1}$  at a  
135 resolution of 4  $\text{cm}^{-1}$ .

136

#### 137 **2.4 Fractionation of chitosan solution**

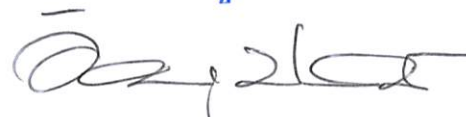
138 Fractionation of chitosan solution was conducted in order to determine the  
139 amount of water-soluble and water-insoluble chitosan of plasma-treated and untreated  
140 samples. In short, the pH of plasma-treated and untreated samples was adjusted to  
141 approximately 7.5 using NaOH solution. The precipitated chitosan was then removed  
142 by centrifuging at 5,000 rpm for 30 minutes. The obtained sample was coded as the  
143 first precipitate (water-insoluble chitosan). The supernatant was then mixed with an  
144 equal volume of acetone to give a second precipitate (water-soluble chitosan). The  
145 first and second precipitate chitosan samples were dried at 60 $^\circ\text{C}$  for 24 hr. The %  
146 yields of the first and second precipitate were calculated following equation 1:

147

$$148 \quad \% \text{yield} = (W_1/W_2) * 100 \quad (1)$$

149

สำเนาถูกต้อง



150 where  $W_1$  and  $W_2$  are the weights of dried precipitate chitosan and the chitosan added  
151 to acetic acid (untreated chitosan), respectively.

152

### 153 3. Results and discussion

154

#### 155 3.1 The effects of types of electrodes on reactive species generated during 156 plasma treatment

157 The emission spectra of plasma-treated chitosan solution, determined at a  
158 treatment time of 1 min, as a function of type of electrodes compared, are presented in  
159 Figure 2. The spectrum of the plasma-treated chitosan solution using W electrode  
160 showed strong peaks at wavelengths of 456.0, 656.5, and 777.3 nm, corresponding to  
161  $H\gamma$ -,  $H\alpha$ -, and O-radicals, respectively (Baroch et al., 2008). These reactive species  
162 could be generated by the decomposition of water molecules, the medium used in this  
163 study, caused by ionic current (Watthanaphanit et al., 2014). After Cu and Fe  
164 electrodes were introduced, the additional spectrum peaks were observed. In the case  
165 of Cu electrodes, the peaks were present at the wavelengths of 324.5 and 521.8 nm,  
166 corresponding to Cu I, while the Fe electrode displayed the peaks at the wavelengths  
167 of 259.9 and 425.0 nm, corresponding to Fe II (Chaves et al., 2011; Tepe et al., 1997).  
168 The presence of Cu I and Fe II species could be attributed to the erosion of copper and  
169 iron particles or ions from each electrode during solution plasma treatment. As  
170 previously reported that the erosion resistance of the Cu and Fe electrodes is relatively  
171 low compared to that of W, the release of material from electrodes was performed and  
172 sputtered by electrolysis (Potocký et al., 2009).

173

174

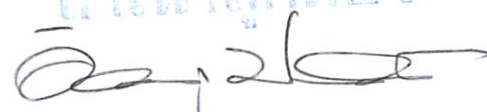
ผู้แทนภาคต่อ  



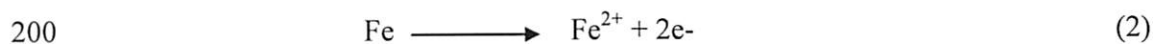

175 **3.2 The effects of type of electrodes and pulse frequency on molecular weight**  
176 **and degradation rate of chitosan**

177 Table 1 shows the change in apparent molecular weight and polydispersity  
178 index (PDI) of chitosan samples during degradation by solution plasma treatment.  
179 From the GPC results, the apparent molecular weight of untreated chitosan was  
180 determined to be  $1.3 \times 10^5$  Da. After solution plasma treatment using the W electrode  
181 for 210 minutes, the molecular weight of chitosan sample was markedly decreased  
182 from the initial value to  $3.1 \times 10^4$  Da. This result corresponded with our previous study  
183 and suggested that degradation of chitosan was occurred during plasma treatment. The  
184 free radicals such as hydroxyl which is performed during plasma treatment  
185 predominantly caused degradation of chitosan (Prasertsung et al., 2011; Prasertsung et  
186 al., 2013). After the Cu and Fe electrodes were employed for the degradation of  
187 chitosan by solution plasma treatment, the degradation reaction was dramatically  
188 enhanced. As shown in Table 1, the molecular weight of the degraded chitosan  
189 products was found to be  $2.4 \times 10^4$  Da for Cu electrodes and  $1.3 \times 10^4$  Da for Fe  
190 electrodes, respectively. Interestingly, the molecular weight of the degraded chitosan  
191 sample treated by solution plasma using Fe electrode was much lower than that of W  
192 and Cu electrodes and was considered to be low molecular weight chitosan (molecular  
193 weight in the range of 5–20 kDa) (Harish Prashanth & Tharanathan, 2007). A stronger  
194 promoting effect from the use of Fe electrodes could be attributed to the iron particle  
195 or ion, which was generated by erosion of the iron electrode via electrolysis during  
196 plasma treatment, as noted in Figure 2. These particles or ions could be transformed  
197 into ferrous ion by oxidation at the electrode during solution plasma treatment as  
198 follows (Sarahney et al., 2012):

199

อำนาจด้อย  


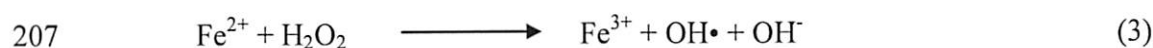




201

202 As previously reported by Chang *et al.* (Chang et al., 2011), the ferrous ion  
 203 could enhance the Fenton reaction which decomposes the H<sub>2</sub>O<sub>2</sub> generated in the  
 204 system during solution plasma treatment and provided high amounts of hydroxyl  
 205 radicals as follows:

206



209

210 Therefore, the decomposition of H<sub>2</sub>O<sub>2</sub> by Fenton reaction may also be  
 211 responsible for a decrease in the molecular weight of degraded products. Moreover,  
 212 the generated iron particles could react with chitosan to form the chitosan–metal  
 213 complex by the interaction of OH and NH<sub>2</sub> groups on the chitosan structure. This led  
 214 to an enhanced degradation of chitosan, since the polymeric chitosan chain in the  
 215 chitosan-metal complex was broken down more easily than that of chitosan itself  
 216 (Pornsunthorntawee et al., 2014).

217 Considering the effects of pulse frequency on molecular weight reduction, as  
 218 shown in Table 1, it was observed that the molecular weight of the degraded product  
 219 decreased with increasing pulse frequency. The molecular weight of chitosan after  
 220 plasma treatment at the applied pulse frequencies of 15 kHz, 22.5 kHz, and 30 kHz  
 221 were measured to be 1.3x10<sup>4</sup> Da, 9.2x10<sup>3</sup> Da, and 6.8x10<sup>3</sup> Da, respectively. The  
 222 greater improvement in the molecular weight reduction at high pulse frequency could  
 223 be attributed to the energy input increased when the pulse frequency increased, as  
 224 previously reported by Kang *et al.* (Kang et al., 2013). The increase in energy input

สำนักวิทยบริการ  
 มหาวิทยาลัยเทคโนโลยีพระจอมเกล้าธนบุรี

๐๒/๒๕๖๕

225 could enhance the amount of hydroxyl radical during solution plasma treatment. This  
 226 could promote the degradation process of chitosan caused by plasma treatment,  
 227 resulting in a high rate constant of the degradation reaction.

228 According to the results of molecular weight reduction, the degradation  
 229 kinetics was then analyzed based on the relationship between the apparent molecular  
 230 weight ( $M_w$ ) of the chitosan sample and the reaction time as follows  
 231 (Pornsunthorntawee et al., 2014):

232

$$233 \quad \frac{1}{M_t} = \frac{1}{M_0} + \frac{kt}{M} = \frac{1}{M_0} + \dot{k}t \quad (5)$$

234

235 where  $M_t$  is  $M_w$  of chitosan sample at reaction time ( $t$ ),  $M_0$  is the initial  $M_w$  of the  
 236 chitosan sample,  $M$  is the molecular weight of the chitosan monomer,  $k$  ( $\text{min}^{-1}$ ) or  $\dot{k}$   
 237 ( $\text{gmol}^{-1} \cdot \text{min}^{-1}$ ) is the degradation rate constant, and  $t$  is the reaction time. Figure 3  
 238 shows a linear relationship between the chitosan molecular weight and reaction time  
 239 for the degradation of chitosan by solution plasma (reaction time between 0 min to  
 240 210 min). The  $k$  value of the degradation of chitosan by solution plasma using the W  
 241 electrode was determined to be  $3.77 \times 10^{-2} \text{ min}^{-1}$ . After Cu and Fe electrodes were  
 242 introduced, the  $k$  values of degradation of chitosan were calculated to be  $5.66 \times 10^{-2}$   
 243  $\text{min}^{-1}$  and  $1.22 \times 10^{-1} \text{ min}^{-1}$ , respectively. The obtained  $k$  value for the solution plasma  
 244 treatment using Cu and Fe were higher than for the W electrode. Our results are  
 245 consistent with those reported by Pornsunthorntawee *et al.*, who studied  
 246 depolymerization of the chitosan-metal complex via solution plasma. They suggested  
 247 that the addition of  $\text{Cu}^{2+}$  and  $\text{Fe}^{2+}$  ions into chitosan solution could strongly promote  
 248 the degradation rate of chitosan (Pornsunthorntawee et al., 2014). Considering the  
 249 effect of pulse frequency on degradation rate, it was found that the  $k$  value of chitosan

สำนักวิทยบริการ  
 อ. 2/25

250 degradation was increased with increasing pulse frequency. The  $k$  values of chitosan  
251 degradation treated by solution plasma at pulse frequency of 22.5 kHz and 30 kHz  
252 were calculated to be  $1.77 \times 10^{-1} \text{ min}^{-1}$  and  $2.39 \times 10^{-1} \text{ min}^{-1}$ , respectively. Based on the  
253 calculation of  $k$ , the order of degradation reaction of chitosan by solution plasma was  
254 evaluated to be Fe at 30 kHz ( $2.39 \times 10^{-1} \text{ min}^{-1}$ )  $\sim$  Fe at 22.5 kHz ( $1.77 \times 10^{-1} \text{ min}^{-1}$ )  $>$  Fe  
255 at 15 kHz ( $1.22 \times 10^{-1} \text{ min}^{-1}$ )  $>$  Cu at 15 kHz ( $5.66 \times 10^{-2} \text{ min}^{-1}$ )  $\gg$  W at 15 kHz  
256 ( $3.77 \times 10^{-2} \text{ min}^{-1}$ ). Therefore, our results clarified that the solution plasma treatment  
257 using Fe electrode at high pulse frequency is an effective condition for degradation of  
258 chitosan. Moreover, the calculated  $k$  of the chitosan degradation by the solution  
259 plasma treatment using Fe electrodes was much higher than those previously reported  
260 in the literature. For example, the  $k$  value of the enzymatic degradation of chitosan  
261 and chitosan degradation in the presence of  $\text{H}_2\text{O}_2$  was reported to be in the range of  
262  $10^{-5}$ – $10^{-4} \text{ min}^{-1}$  (Chang et al., 2001; Ilyina et al., 2000). This was approximately 2–3  
263 orders of magnitude lower than our results.

264

### 265 3.3 XRD analysis

266 The X-ray diffraction patterns of plasma-treated and untreated chitosan are  
267 shown in Figure 4. It was observed that the untreated chitosan sample displayed a  
268 crystal structure with two characteristic peaks at  $2\theta = 15.1^\circ$  and  $21.4^\circ$ , which is  
269 referred to as the mixture of the “tendon hydrate polymorph” and “annealed  
270 polymorph” (Ogawa, 1991). After plasma treatment using the W electrode for 210  
271 minutes, the diffraction peak located at a  $2\theta$  of  $15.1^\circ$  disappeared while the peak  
272 located at a  $2\theta$  of  $21.4^\circ$  became broader. This suggested that the crystalline region of  
273 the chitosan sample was destroyed during plasma treatment. When the Cu electrode  
274 was applied, the diffraction peak at  $2\theta$  equal to  $15.1^\circ$  in the XRD patterns of the

ศาสตราจารย์  
อ.ดร.วิมลรัตน์




275 degraded chitosan products still disappeared but the peak at a  $2\theta$  of  $20^\circ$  was much  
276 broader with a much lower peak intensity. Interestingly, it was observed that after the  
277 chitosan was treated with plasma using the Fe electrode at the pulse frequency of 15  
278 kHz and 30 kHz, the diffraction peak located at a  $2\theta$  of  $15.1^\circ$  and  $21.4^\circ$  disappeared.  
279 These results revealed that the solution plasma treatment of chitosan using Fe  
280 electrodes could disrupt the crystalline structure of the chitosan sample more than W  
281 and Cu electrodes. This corresponds to the results regarding the degradation rate of  
282 chitosan, as shown in Figure 3. An increase in disruption of the crystal structure of  
283 chitosan could improve an accessibility of hydroxyl radicals generated by plasma  
284 treatment, which enhanced the degradation process, and finally resulted in an  
285 increased degradation rate of chitosan.

286

### 287 3.4 FT-IR spectra

288 The FT-IR spectra of plasma-treated and untreated chitosan samples are  
289 shown in Figure 5. It was demonstrated that the characteristic peaks of untreated  
290 chitosan films appeared at  $1668$ ,  $1558$  and  $1152\text{ cm}^{-1}$ , which corresponded to C=O  
291 stretching,  $\text{-NH}_2$  bending, and  $\text{-C-O-C-}$  glycosidic linkage between chitosan monomer,  
292 respectively (Pornsunthorntawee et al., 2014; Li et al., 2012). After being treated with  
293 solution plasma, no additional characteristic peak was observed in the FTIR spectra of  
294 the degraded products. The characteristic peaks of plasma-treated chitosan mostly  
295 exhibited the same bands as the untreated sample. This indicated that the main  
296 polysaccharide structure of degraded chitosan remains unchanged. The degradation of  
297 chitosan by solution plasma treatment did not modify the chemical structure of  
298 chitosan. However, some differences between the chitosan products treated by  
299 solution plasma using Fe electrodes at both pulse frequency of 15 kHz and 30 kHz

ศาสตราจารย์ ดร. อรุณรัตน์





300 and untreated chitosan samples were observed in the range of 1300-1600  $\text{cm}^{-1}$ . The  
301 bands at 1410  $\text{cm}^{-1}$  (symmetrical deformation of  $\text{CH}_3$  and  $\text{CH}_2$ ) and 1370  $\text{cm}^{-1}$   
302 (bending and stretching of  $\text{CH}_3$  and  $\text{CH}_2$ ) were weakened. This implied that the  
303 intermolecular hydrogen bonding of plasma-treated chitosan was decreased.  
304 Moreover, its crystallinity was reduced during plasma treatment (Li et al., 2005).

305

### 306 3.5 Fractionation of chitosan samples

307 Figure 6 shows the %yield of water-soluble and water-insoluble, as well as the  
308 total %yield, of chitosan samples as a function of type electrode and applied pulse  
309 frequency. The %yield of water-soluble chitosan (second precipitate) of the chitosan  
310 product after plasma treatment using W and Cu electrodes were measured to be 26%  
311 and 30%, respectively. When the Fe electrode was applied, the %yield of water-  
312 soluble chitosan increased greatly up to 60%. This result is also consistent with the  
313 calculated rate constant of the degradation reaction of the chitosan sample. This  
314 revealed that the solution plasma treatment of chitosan using Fe electrodes could  
315 induce the degradation of chitosan to obtain the highest amount of water-soluble  
316 chitosan products. However, some water-insoluble chitosan samples appeared in the  
317 degraded product. This might be a result of the non-uniformity and non-specific  
318 cleavage of degradation processes of chitosan by solution plasma treatment.  
319 Considering the effect of pulse frequency on chitosan products, it was found that  
320 the %yield of water-soluble chitosan products did not change when the pulse  
321 frequency was increased. This suggested that an increase in pulse frequency had an  
322 effect on the degradation rate but not the degraded chitosan product, i.e. the amount of  
323 water-soluble chitosan.

324

สำเนาถูกต้อง  
[Signature]

325

326 **4. Conclusion**

327 In this study, a solution plasma system was introduced to treat  $\beta$ -chitosan  
328 solutions. The apparent molecular weight of plasma-treated chitosan solutions was  
329 decreased with increasing plasma treatment time, compared to that of an untreated  
330 sample. The degradation rate was greatly affected by the types of electrodes and the  
331 applied pulse frequency. The plasma treatment of chitosan using Fe electrode and  
332 high pulse frequency strongly promoted the degradation rate of chitosan. The  
333 degradation process of chitosan caused by plasma treatment has an effect on the  
334 molecular weight and crystal structure but not chemical structure of chitosan. We also  
335 found that solution plasma treatment of chitosan using Fe electrodes provided the  
336 highest %yield of water-soluble chitosan products compared to those W and Cu  
337 electrodes. These results implied that the Fe was suitable electrode for degradation of  
338 chitosan by solution plasma treatment.

339

340 **Acknowledgements**

341 The solution plasma apparatus supported from EcoTopia Science Institute and  
342 the Technology and Department of Materials Engineering, Nagoya University and the  
343 financial support from Naresuan University (Grant numbers R2558C057) are  
344 gratefully acknowledged.

345

346

347

348

349

สำเนาถูกต้อง  


350 **References**

- 351 Baroch, P., Anita, V., Saito, N., & Takai, O. (2008). Bipolar pulsed electrical  
352 discharge for decomposition of organic compounds in water. *J. Electrostat.*, 66,  
353 294-299.
- 354 Chang, K.L.B., Tai, M.C., & Cheng, F.H. (2001). Kinetics and products of the  
355 degradation of chitosan by hydrogen peroxide. *J. Agric. Food Chem.*, 49, 4845-  
356 4851.
- 357 Chaves, E.S., de Loos-Vollebregt, M.T., Curtius, A.J., & Vanhaecke, F. (2011).  
358 Determination of trace elements in biodiesel and vegetable oil by inductively  
359 coupled plasma optical emission spectrometry following alcohol dilution.  
360 *Spectrochim. Acta B.*, 66, 733-739.
- 361 Choi, S.W., Ahn, J.K., Lee, W.D., Byun, W.M., & Park, J.H. (2002). Preparation of  
362 chitosan oligomer by irradiation. *Polym. Degrad. Stabil.*, 78, 533-538.
- 363 Harish Prashanth, K.V., & Tharanathan, R. N. (2007). Chitin/chitosan: Modifications  
364 and their unlimited application potential – An overview. *Trens. Food Sci. Tech.*,  
365 18, 117–131.
- 366 Ilyina, A.V., Tikhonov, V.E., Albulov, A.I., & Varlamov, V.P. (2000). Enzymatic  
367 preparation of acid-free-water-soluble chitosan. *Process Biochem.*, 35, 563-568.
- 368 Jayakumar, R., Menon, D., Manzoor, K., Nair, S.V., & Tamura, H. (2010).  
369 Biomedical applications of chitin and chitosan-based nanomaterials-A Short  
370 Review. *Carbohydr. Polym.*, 82(2), 227-232.
- 371 Jayakumar, R., Prabakaran, M., Sudheesh, Kumar, P.T., Nair, S.V., & Tamura, H.  
372 (2011). Biomaterials based on chitin and chitosan in wound dressing  
373 applications. *Biotechnol. Adv.*, 29(3), 322-337.

สำเนาถูกต้อง



- 374 Kang, J., Li, O.L., & Saito, N. (2013). Synthesis of structure-controlled carbon nano  
375 spheres by solution plasma process. *Carbon*, 60, 293-298.
- 376 Li, J., Du, Y., Yang, J., Feng, T., Li, A., & Chen, P. (2005). Preparation and  
377 characterization of low molecular weight chitosan and chito-oligomers by a  
378 commercial enzyme. *Polym. Degrad. Stabil.*, 87, 441-448.
- 379 Li, K., Xing, R., Liu, S., Qin, Y., Meng, X., & Li, P. (2012). Microwave-assisted  
380 degradation of chitosan for a possible use in inhibiting crop pathogenic fungi.  
381 *Int. J. Biol. Macromol.*, 51, 767-773.
- 382 Ogawa, K. (1991). Effect of heating an aqueous suspension of chitosan on the  
383 crystallinity and polymorphs. *Agric. Biol. Chem.*, 55, 2375-2379.
- 384 Pornsunthorntawee, O., Katepetch, C., Vanichvattanadecha, C., Saito, N., &  
385 Rujiravanit, R. (2014). Depolymerization of chitosan-metal complexes via a  
386 solution plasma technique. *Carbohydr. Polym.*, 102, 504-512.
- 387 Potocký, Š., Saito, N., & Takai, O. (2009). Needle electrode erosion in water plasma  
388 discharge. *Thin Solid Films.*, 518, 918-923.
- 389 Prasertsung, I., Damrongsakkul, S., Terashima, C., Saito, N., & Takai, O. (2011).  
390 Preparation of low molecular weight chitosan using solution plasma system.  
391 *Carbohydr. Polym.*, 87, 2745-2749.
- 392 Prasertsung, I., Damrongsakkul, S., & Saito, N. (2013). Degradation of  $\beta$ -chitosan by  
393 solution plasma process. *Polym. Degrad. Stabil.*, 98, 2089-2093.
- 394 Sarahney, H., Mao, X., & Alshawabkeha, A.N. (2012). Role of iron anode oxidation  
395 on transformation of chromium by Electrolysis. *Electrochim Acta.*, 86, 96-101.
- 396 Sashiwa, H., Fujishima, S., Yamano, N., Kawasaki, N., Nakayama, A., Muraki, E.,  
397 Sukwattanasinitt, M., Pichyangkura, R., & Aiba, S. (2003). Enzymatic  
398 production of N-acetyl-D-glucosamine from chitin: Degradation study of N-

สำเนาถูกต้อง





- 399 acetylchitooligosaccharide and the effect of mixing of crude enzyme. *Carbohydr.*  
400 *Polym.*, 51, 391-395.
- 401 Shahidi, F., Arachchi, J.K.V., & Jeon, Y.J. (1999). Food applications of chitin and  
402 chitosans. *Trends. Food. Sci. Technol.*, 10(2), 37-51.
- 403 Takai, O. (2008). Solution plasma processing (SPP). *Pure Appl. Chem.*, 80, 2003-  
404 2011.
- 405 Tepe, R.K., Jacksier, T., & Barnes, R.M. (1997). Atomic emission of anhydrous  
406 hydrogen bromide: spectra from 200 to 900 nm by sealed inductively coupled  
407 plasma-atomic emission spectroscopy. *Spectrochim. Acta B.*, 52, 2103-2113.
- 408 Watthanaphanit, A., Heo, Y.K., & Saito, N. (2014). Influence of the discharge time of  
409 solution plasma process on the formation of gold nanoparticles in alginate  
410 matrix. *J. Taiwan Inst. Chem. E.*, 45, 3099-3103.
- 411 Xie, Y., Hu, J., Wei, Y., & Hong, X. (2009). Preparation of chitooligosaccharides by  
412 the enzymatic hydrolysis of chitosan. *Polym. Degrad. Stabil.*, 94, 1895-1899.
- 413 Yue, W., Yoa, P., Wei, Y., & Mo, H. (2008). Synergetic effect of ozone and  
414 ultrasonic radiation on degradation of chitosan. *Polym. Degrad. Stabil.*, 93,  
415 1814-1821.
- 416
- 417

สำเนาถูกต้อง  


### Figure captions

- Figure 1. Schematic diagram of solution plasma process.
- Figure 2. OES spectrum of plasma-treated chitosan solution (chitosan concentration and treatment time of 0.5% w/v and 1 min, respectively).
- Figure 3. Linear relationship between the inverse of the molecular weight ( $1/M_t$ ) and the degradation time (t) for the degradation of the chitosan by solution plasma.
- Figure 4. X-ray diffraction patterns of plasma-treated and untreated chitosan.
- Figure 5. FT-IR spectra of plasma-treated untreated and chitosan films.
- Figure 6. %yield of water-insoluble chitosan, water-soluble chitosan, and total yield of degraded products obtained from solution plasma of chitosan.

### Table caption

- Table 1. Weight average molecular weight ( $M_w$ ) and polydispersity index (PDI) of a chitosan sample after degradation by solution plasma process in a 0.5% (w/v) acetic acid solution using various types of electrodes and applied pulse frequency at 15-30 kHz.

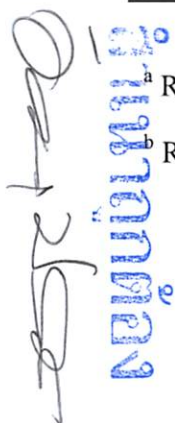
สำเนาถูกต้อง  
อ. 2/56

Table 1. Prasertsung, et al.

Reaction Time (min)	Molecular weight (Da)/(PDI)				
	Types of electrodes (Applied pulse frequency)				
	W (15 kHz)	Cu (15 kHz)	Fe (15 kHz)	Fe (22.5 kHz)	Fe (30 kHz)
0	1.3x10 <sup>5a</sup> (3.5) <sup>b</sup>	1.3x10 <sup>5</sup> (3.5)	1.3x10 <sup>5</sup> (3.5)	1.3x10 <sup>5</sup> (3.5)	1.3x10 <sup>5</sup> (3.5)
60	8.7x10 <sup>4</sup> (2.9)	6.2x10 <sup>4</sup> (3.0)	4.1x10 <sup>4</sup> (2.8)	3.0x10 <sup>4</sup> (3.5)	2.6x10 <sup>4</sup> (3.5)
120	6.4x10 <sup>4</sup> (2.9)	4.3x10 <sup>4</sup> (2.8)	2.0x10 <sup>4</sup> (2.5)	1.5x10 <sup>4</sup> (3.2)	1.2x10 <sup>4</sup> (3.0)
210	3.1x10 <sup>4</sup> (2.7)	2.4x10 <sup>4</sup> (2.5)	1.3x10 <sup>4</sup> (2.3)	9.2x10 <sup>3</sup> (2.8)	6.8x10 <sup>3</sup> (2.7)

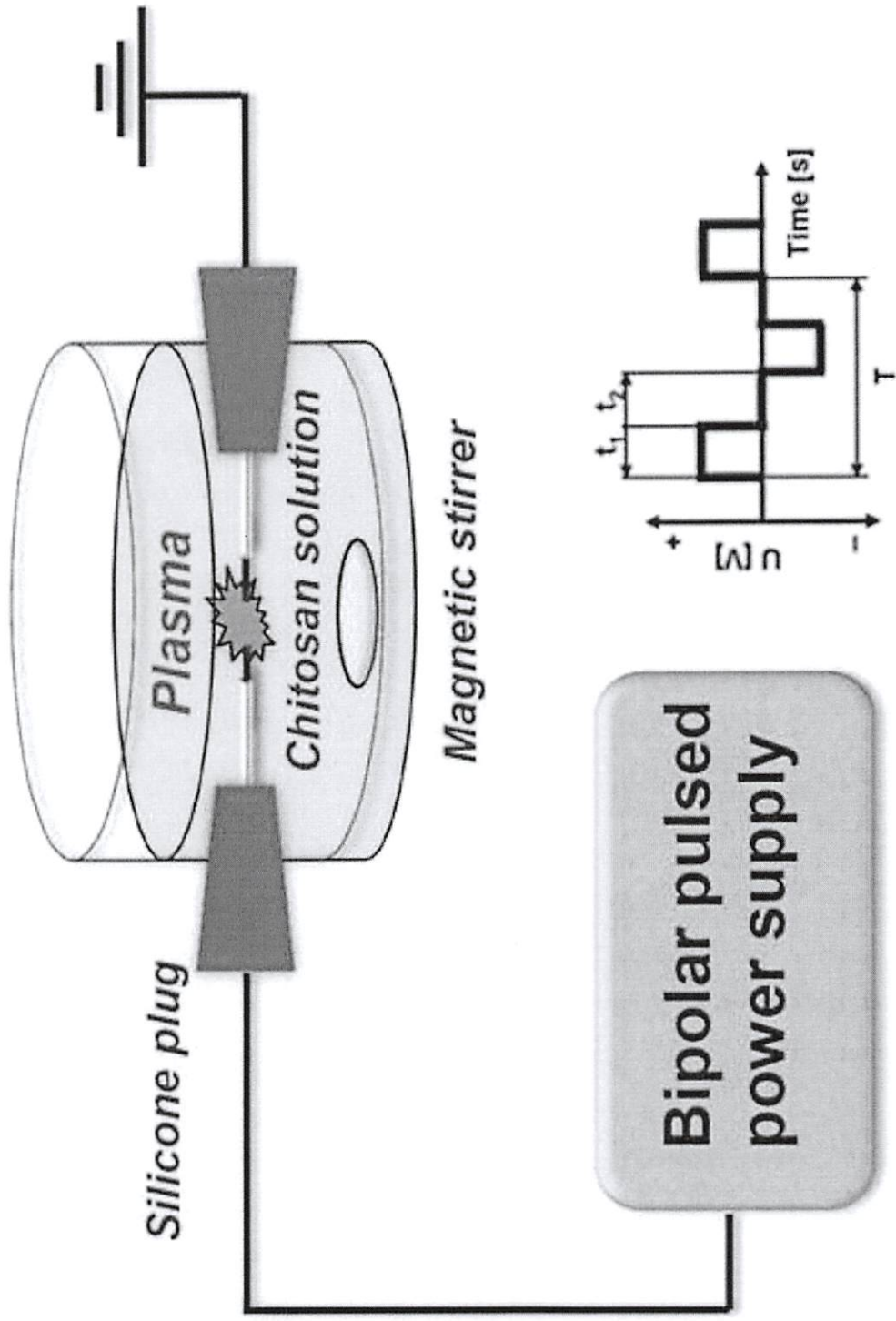
<sup>a</sup> Reported values are M<sub>w</sub> of the chitosan sample.

<sup>b</sup> Reported values are the PDI of the chitosan sample.



Handwritten signature and a blue stamp with Thai text.

Figure1  
Click here to download high resolution image

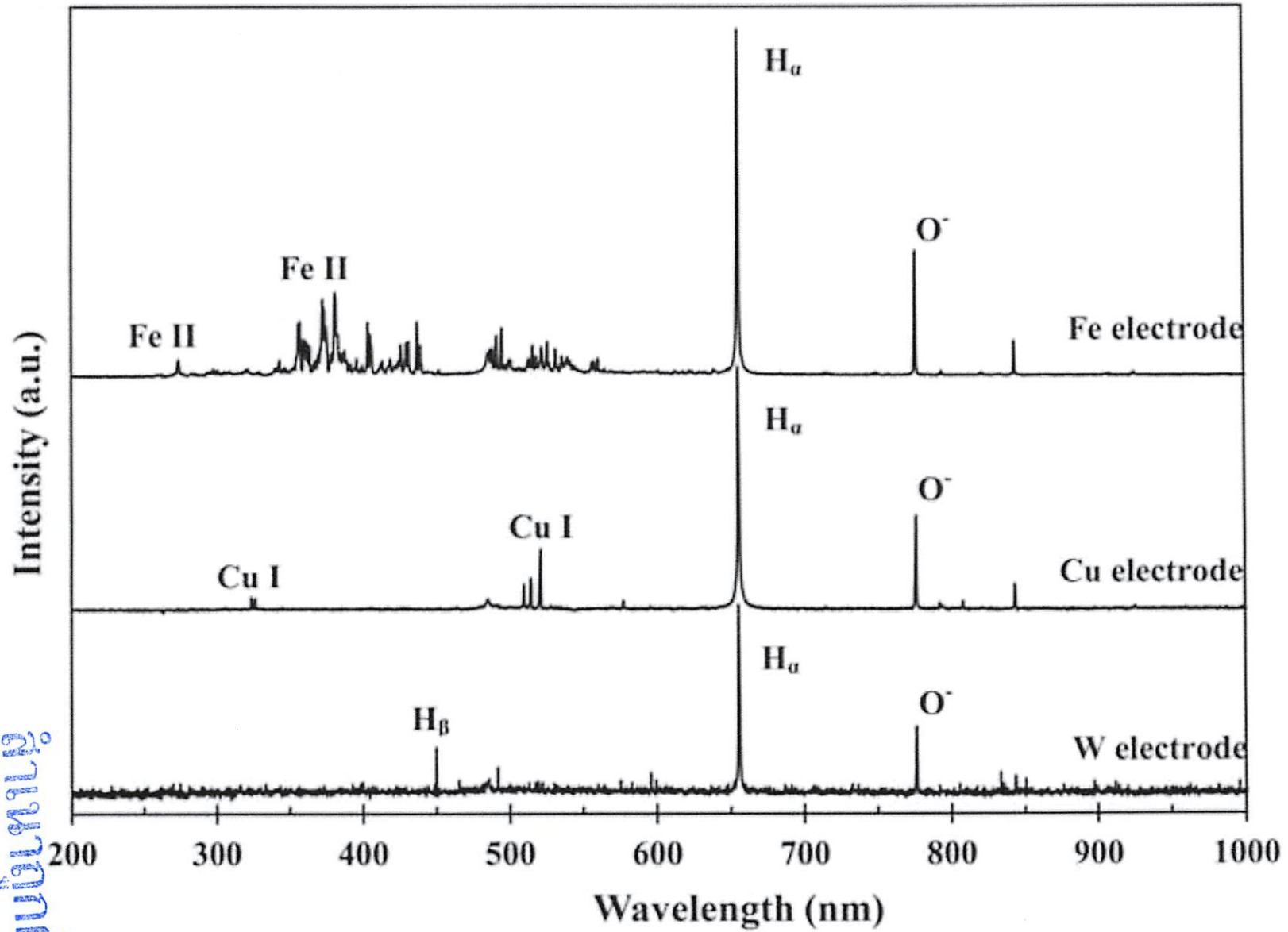


จำนวนมากต้อง  
[Signature]

Figure 1. Prasertsung, et al.



Figure2  
Click here to download high resolution image



Handwritten signature and blue text:   
Handwritten signature: *[Signature]*  
Blue text: **www.ijer.org**

Figure 2. Prasertsung, et al.

Figure3

[Click here to download high resolution image](#)

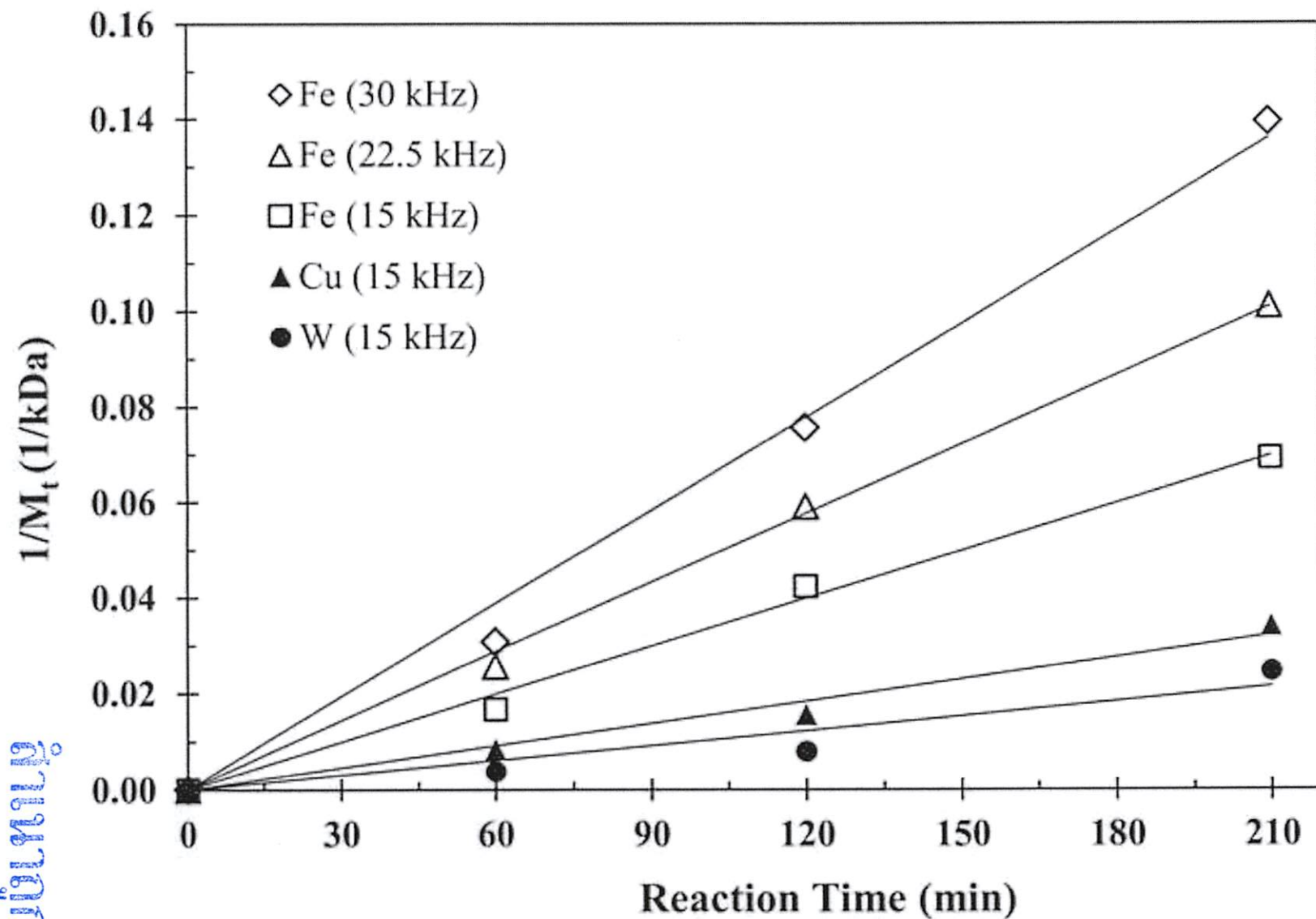


Figure 3. Prasertsung, et al.

Prasertsung  
et al.

Figure4  
Click here to download high resolution image

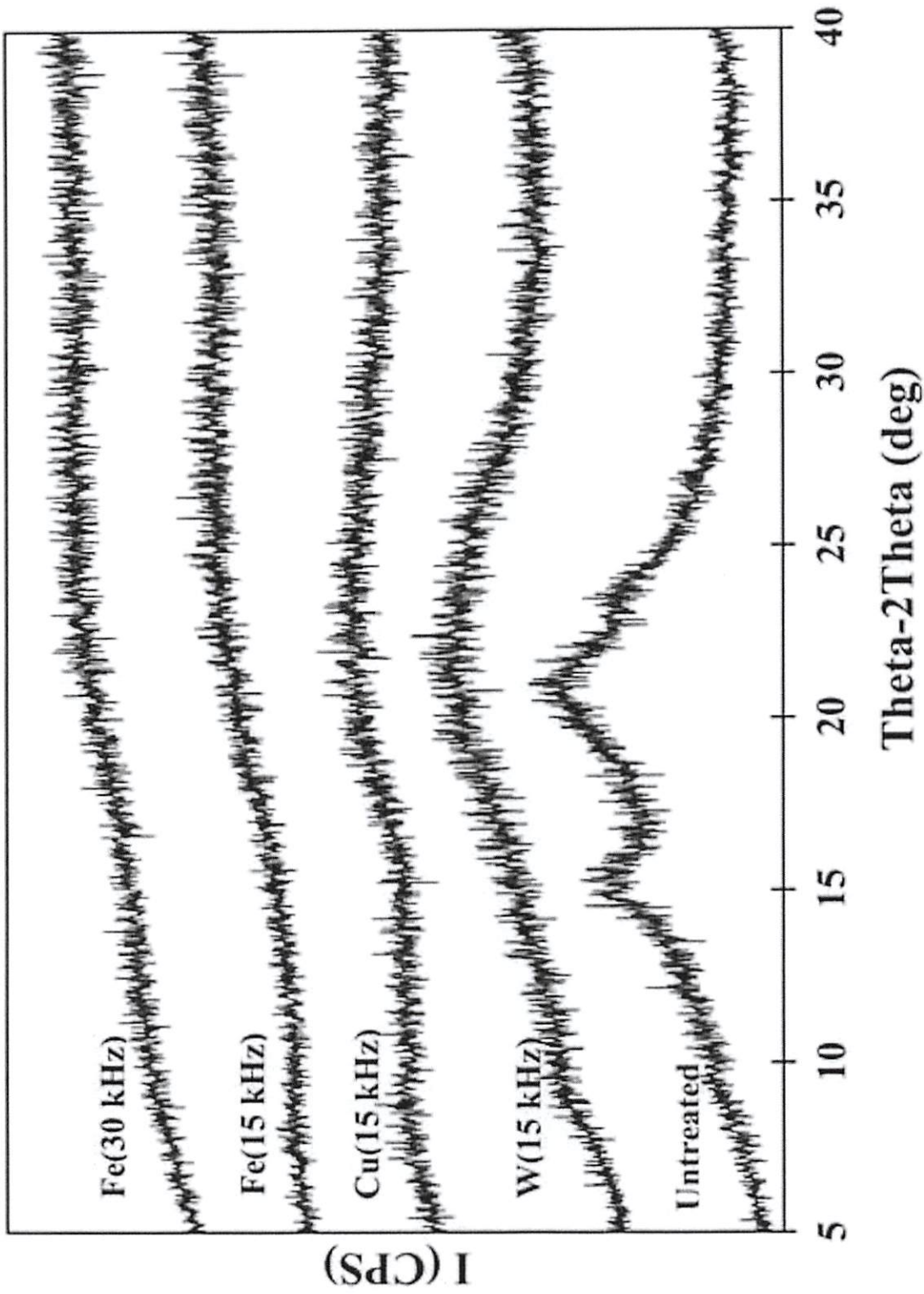


Figure 4. Prasertsung, et al.

สำเนาถูกต้อง  


Figure5  
[Click here to download high resolution image](#)

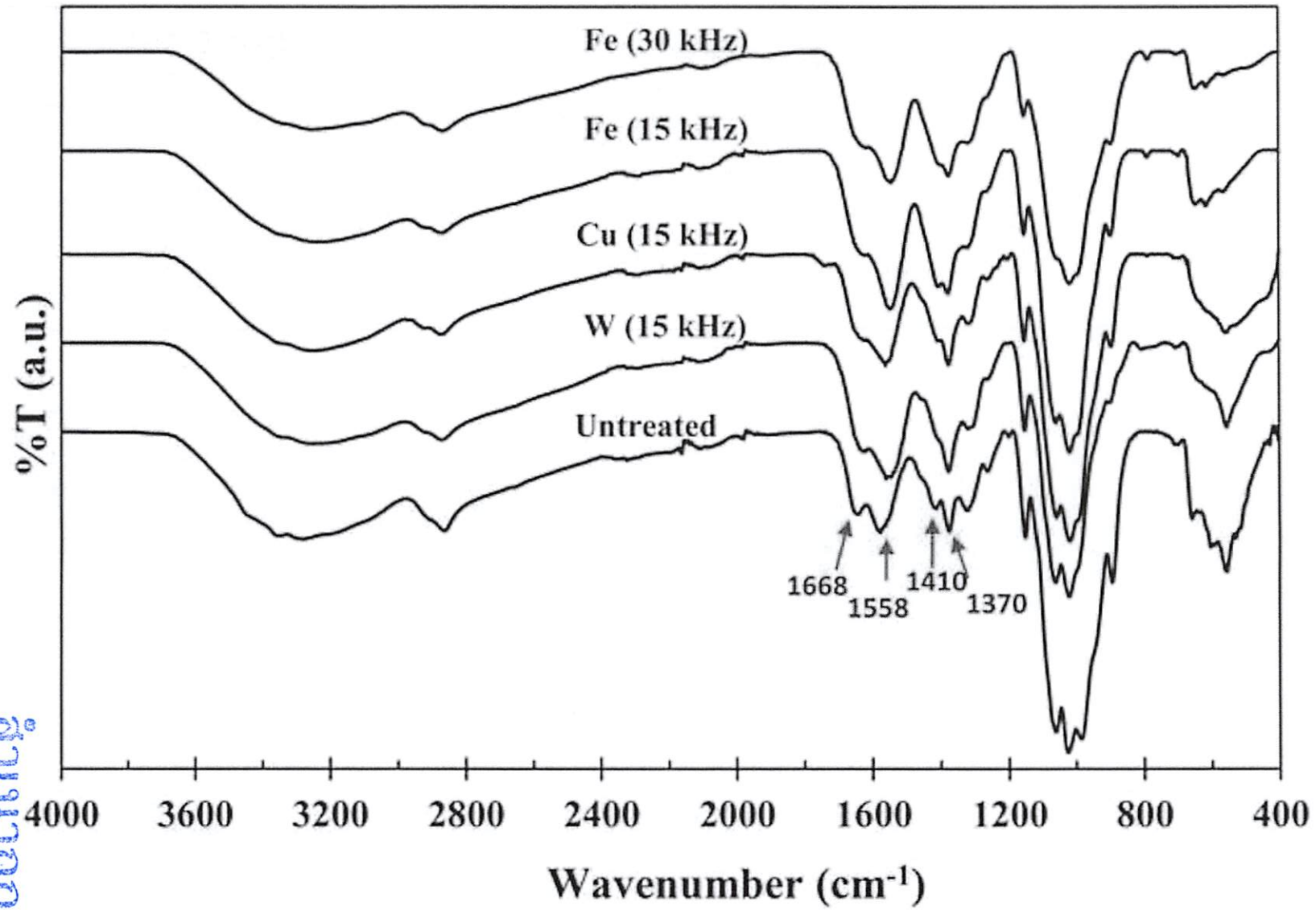


Figure 5. Prasertsung, et al.

Handwritten signature and blue text: **Prasertsung**



Figure6  
Click here to download high resolution image

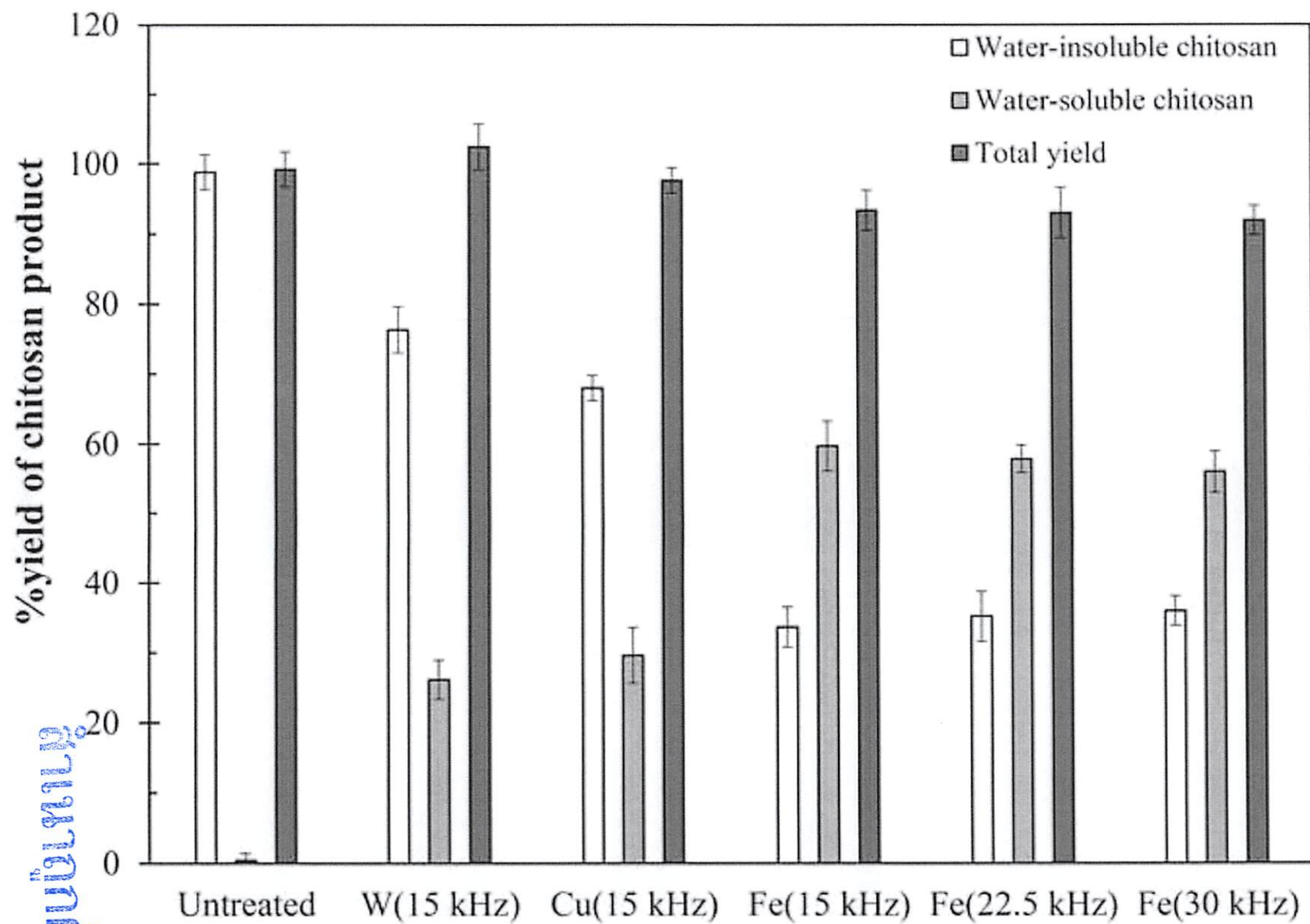


Figure 6. Prasertsung, et al.

*Prasertsung*

Prasertsung